Analysis of Linear Cooperative Multi-hop Networks Subject to Correlated Shadowing and Composite Shadowing-Fading

By

Mudasar Bacha

2010-NUST-MS-CSE(S)-13

Supervisor

Dr. Syed Ali Hassan

Department of Electrical Engineering

A thesis submitted in partial fulfillment of the requirements for the degree of Masters in Communication Systems Engineering (MS CSE)

In

School of Electrical Engineering and Computer Science,

National University of Sciences and Technology (NUST),

Islamabad, Pakistan.

(February 2013)

Approval

It is certified that the contents and form of the thesis entitled "**Analysis of Linear Cooperative Multi-hop Networks Subject to Correlated Shadowing and Composite Shadowing-Fading**" submitted by **Mudasar Bacha** have been found satisfactory for the requirement of the degree.

Advisor: **Dr. Syed Ali Hassan**

Signature: _____

Date: _____

Committee Member 1: **Dr. Adnan Khalid Kiani**

Signature: _____

Date: _____

Committee Member 2: **Dr. Khawar Khurshid**

Signature: _____

Date: _____

Committee Member 3: **Dr. Zawar Hussain Shah**

Signature: _____

Date: _____

Abstract

We develop a stochastic model to characterize the effects of both correlated shadowing and composite shadowing-fading. We consider a cooperative multi-hop line network, where a group of nodes cooperatively transmits the same message to another group of nodes, and model the transmission from one group to another as a discrete-time quasi-stationary Markov process. We derive the transition probability matrix of the Markov chain by first considering the wireless channel exhibiting shadow fading and then composite shadowing-fading. The shadowing is modeled as a log-normal random variable (RV) while the composite shadowing-fading is modeled as Suzuki (Rayleigh-lognormal) RV. We use Fenton-Wilkinson method to approximate the sum distribution of the multiple correlated log-normal RVs to a single log-normal RV, while in order to find the sum distribution of the multiple independent Suzuki RVs to a single log-normal RV, we use a moment generating function (MGF)-based approximation technique. This MGF-based technique uses Gauss-Hermite integration to present the sum distribution in closed form. We quantify the signal-to-noise ratio (SNR) margin required to achieve a certain quality of service (QoS) under standard deviation of the shadowing. The effect of increasing standard deviation of the shadowing on the network coverage is also quantified. We also provide the optimal level

of cooperation required for obtaining maximum coverage of a line network under a given QoS. Two topologies for linear network are considered and the performance of each topology under various system parameters is provided. The analytical results have been validated by matching with the simulation results.

Certificate of Originality

I hereby declare that this submission is my own work and to the best of my knowledge it contains no materials previously published or written by another person, nor material which to a substantial extent has been accepted for the award of any degree or diploma at NUST SEECS or at any other educational institute, except where due acknowledgement has been made in the thesis. Any contribution made to the research by others, with whom I have worked at NUST SEECS or elsewhere, is explicitly acknowledged in the thesis.

I also declare that the intellectual content of this thesis is the product of my own work, except for the assistance from others in the project's design and conception or in style, presentation and linguistics which has been acknowledged.

Author Name: **Mudasar Bacha**

Signature: _____

Acknowledgment

Above all, I am extremely thankful to Almighty Allah, for His countless blessing bestowed on me throughout my life. Without His will and blessing nothing would have been possible.

My profound gratitude to my thesis supervisor Dr. Syed Ali Hassan, for his continuous encouragement, enlightening advice, and most willing help extended by him throughout my research work.

I am also thankful to Dr. Adnan Khalid Kiani, Dr. Khawar Khurshid, and Dr. Zawar Hussain Shah for his their support and time. My special thanks to Dr. Adnan Khalid Kiani for his guidance throughout my MS studies.

I also want to mention the names of my friends, Muhammad Hanif, Junaid Ahmad Khan, Arshad Ali, and Muhammad Aftab for their unconditional support. I am grateful to them.

Last, but by no mean the least, my heartfelt thanks to my Mother and Father, for their unwavering support and encouragement throughout my educational career. I am also thankful to my brothers and sisters for their support and love.

Table of Contents

List of Figures

Chapter 1

Introduction

1.1 Introduction to Cooperative Communication

High data rate is becoming one of the main feature in next generation wireless systems owing to the ever increasing demands for multimedia services and web-related contents. However, the data rate capability of the wireless networks is limited by channel fading and other transmission impairments. In order to combat channel fading, different diversity schemes have been proposed such as time diversity, frequency diversity and spatial diversity. Spatial diversity techniques are mainly attractive because they offer diversity gain without incurring additional costs of transmission time and bandwidth. Spatial diversity is achieved by using multiple antennas at transmitter and receiver called multiple-input multiple-output (MIMO) [1]. Multiple antennas are spaced on the order of a wavelength to avoid the correlation among different transmitted signals. MIMO architectures effectively achieve high

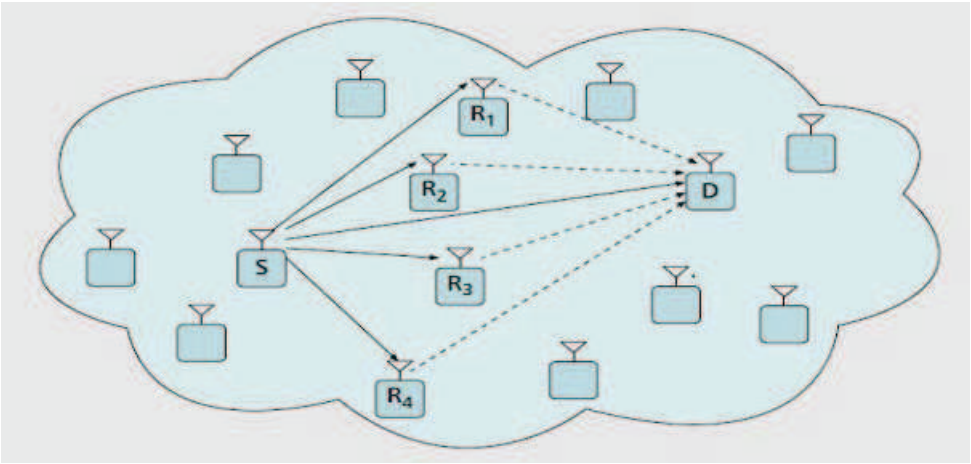

Figure 1.1: Cooperative wireless network

.

system throughput and combat channel fading. However, MIMO system is difficult to implement on small mobile equipments and sensor nodes due to its small size and also the cost will go up with the installment of additional antennas [6].

To overcome the above mentioned problems of MIMO systems, a new technique named distributed MIMO was proposed and has attracted a lot of attention. The key difference between the distributed and co-located MIMO is that multiple antennas at the front end of wireless networks are distributed among widely separated radio nodes. Different nodes at different locations transmit the same data to the receiver. In this way, multiple nodes form a virtual antenna array that achieves higher spatial diversity gain. This kind of communication is called cooperative communication and spatial diversity is called cooperative diversity [2]. This style of cooperative transmission (CT) is becoming popular in the past several years in both sensor and cellular networks. Figure 1.1 shows a cooperative wireless network, where node S wants

to transmit to node D. The intermediate nodes, R_1 to R_4 work as relaying nodes and forward the data to the destination node D. The transmitter and the relays form a virtual antenna array to achieve the spatial diversity [6].

Wireless multi-hop cooperative communications has a wide variety of applications such as in cellular network, sensor network, and wireless computer network. In cellular mobile networks, it is difficult to provide high data rate all over a cell, especially at the cell boundary. One possible solution of this problem is to reduce the size of the cell, which will require additional base stations and can lead to substantial additional costs. The cooperative communication allows an effective and cost-efficient substitute to ensure high data rate at the cell boundary, by enabling the additional nodes to work as a relay between the base station and the mobile user. The cooperative communication can also provide high speed connectivity to residential areas via roof-top relaying systems. This type of communication architecture can provide high data rate connection between base stations without additional hardware such as microwave or optical fiber [5].

The cooperation among nodes not only increase user's capacity but also leads to a more robust system, where user's achievable rates are less vulnerable to channel variations. This increase in data rate due to cooperation can be translated into reduced power for the users. With cooperation, users can achieve a certain rate with less total power. This scheme can also extend battery life of the mobiles. The cooperation gain may be used to increase cell coverage in a cellular system [3]. Cooperative communication can be effectively used to address the energy deficiency issue in the sensor networks [7]. It can also be used for the range extension of the sensor networks [17].

Anna Scaglione and Yao-Win Hong propose an efficient physical layer transmission technique for cooperative communication called Opportunistic Large Array (OLA) [8]. The behavior of dense wireless cooperative networks is studied in [16]. It was shown that if the decoding threshold is below a particular value, the message can be transfered to the receiver irrespective of how far it is. The authors considered an infinite node density per unit area, emitting a constant power from that area. This *continuum* assumption may not be an appropriate candidate for finite density networks, also their work was mainly based on simulation experiments. The authors in [18] studied a finite density cooperative multi-hop line network and found the coverage of the network under multi-path fading. They only considered small-scale fading, however in practical wireless channels both small-scale as well as large-scale fading (shadowing) are present [20].

1.2 Problem Statement

There are three main channel impairments namely, path loss, multipath (small-scale) fading and shadowing (large-scale fading), which distort the received signal in wireless communication system. Path loss is a deterministic process, while multipath and shadowing are random and due to multipath and shadowing the received power of the signal shows random fluctuations. Fig. 1.2. shows the effect of path loss, shadowing and multipath fading on the ratio of received-to-transmit power versus log-distance of the channel [35]. In practical wireless systems, both small-scale as well as large-scale fading are present and affect the system performance [20]. However, according to our literature survey there is no significant work which has considered shad-

owing and composite shadowing-fading for opportunistic large array (OLA) cooperative networks. The authors in [18] studied OLA cooperative networks however, they only considered small-scale fading. Our research problem is to study **the performance of cooperative multi-hop linear network under shadowing and composite shadowing-fading**. We model the shadowing as log-normal distribution and and the composite shadowing-fading as Suzuki distribution. The received signal in a cooperative network at a node is the sum of multiple transmitted signals and each of this signal is affected by small-scale fading as well as shadowing. However, there is no closed-form expression for the probability density function (PDF) of the sum of multiple log-normal and Suzuki random variables (RVs) [20]. In literature, different approximation techniques have been proposed to find the sum distribution of multiple log-normal and Suzuki RVs. We use Fenton-Wilkinson's [24], method to find the sum distribution of the multiple correlated log-normal RVs, while to find the sum distribution of the multiple Suzuki RVs we use the method proposed in [26], which is a moment generation function (MGF)-based technique. Both of these methods approximate the sum distribution to a single log-normal RV.

1.3 Contribution of the Thesis

We develop a stochastic model to study the impact of correlated log-normal shadowing and composite shadowing-fading for cooperative multi-hop line networks. We model the shadowing as log-normal RV, while the composite shadowing-fading as Suzuki (Rayleigh-lognormal) RV. We approximate the sum distribution of the multiple log-normal RVs to single log-normal RV

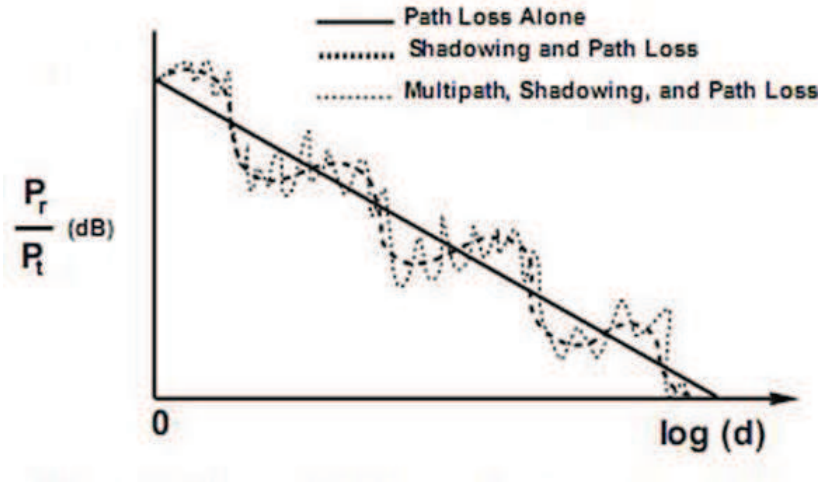

Figure 1.2: Path loss, shadowing and multipath fading versus distance.

by using Fenton-Wilkinson's method. Similarly, we use the moment generation function (MGF)-based technique to approximate the sum distribution of multiple Suzuki RVs to single log-normal RV. We find the coverage of the network under various system parameters such as standard deviation of the shadowing, signal-to-noise ratio (SNR) margin, and path loss. We find the optimal cooperation, which will provide maximum coverage under certain quality-of-service (QoS). We studied the equi-distant and co-located network topologies for line network and find the performance of each topology under various system parameters for composite shadowing-fading. We compare the coverage of the network for three different channel model, i.e., fading, shadowing and composite shadowing-fading channels.

1.4 Thesis Organization

The rest of the thesis is organized as follows, Chapter 2 presents the related work on cooperative network modeling and different approximation techniques used for finding the sum distribution of log-normal and Suzuki RVs. In Chapter 3, we discuss the network model and the assumptions we made. It also discusses the network as a discrete-time quasi-stationary Markov chain. Chapter 4 presents how we approximate the sum of multiple log-normal RVs to a single log-normal RV using Fenton-Wilkinson's method. This chapter also discusses how we find the transition probability matrix of the Markov chain and present different interesting results for shadowing channel. In Chapter 5, we find the PDF of the sum of multiple independent Suzuki RVs by using the MGF-based approximation technique. We also presents interesting results for composite shadowing-fading channel. We compare the performance of two different topologies for cooperative multi-hop line networks i.e., equi-distant and co-located network topologies in Chapter 5. Chapter 6 concludes the thesis and gives some recommendations for the future work.

Chapter 2

Literature Review

2.1 Cooperative Network Modeling

The idea of user cooperation diversity was first proposed by Andrew Sendonaris et al. in 2003 [3, 4]. The quality of service and data rate of the mobile users within the duration of the call are limited by the rapid variation in the channel conditions. Therefore, it requires some type of diversity protection. They, in their pioneering work, showed that cooperation among mobile users not only increases system throughput but also makes the user's achievable data rates less vulnerable to channel variations. Increase in the data rate due to cooperation among mobile user can be translated into reduced power for the users. With cooperation, users can achieve a certain rate with less total power, which can extend the battery life of the mobile users. The cooperation gain may also be used to increase cell coverage in a cellular system.

Anna Scaglione and Yao-Win Hong propose an efficient flooding technique for cooperative communication called Opportunistic Large Array (OLA) [8]. In OLA transmission, a group of nodes under orthogonal fading channels

form a *level* and transmit the same message to another level of nodes. All nodes that decode the message successfully from the previous level nodes, relay the message together. It does not require any medium access or routing overhead. In OLA networks, there is no cluster head and each node decide autonomously. This type of transmission can be used to increase the reliability and range of the networks. OLAs networks have high degree of flexibility and scalability. OLAs have applications in many areas such as mobile networks and sensor networks. OLA networks have attracted a great interest from research community and considerable literature on OLA transmission has appeared, e.g., [9, 10, 11, 12, 13, 14, 15].

The behavior of dense wireless cooperative networks is studied in [16]. It was shown that if the decoding threshold is below a particular value, the message can be transfered to the receiver irrespective of how far it is. The authors considered an infinite node density per unit area, emitting a constant power from that area. However, *continuum* assumption may not be an appropriate candidate for finite density networks, also their work was mainly based on simulation experiments.

The authors in [18] studied a finite density multi-hop cooperative network, which forms Opportunistic Large Array (OLA). They developed an analytical model for a multi-hop cooperative line network. Under fading channel environment, they modeled the received power on a node as a hypoexponential distribution and provided an upper bound on the network coverage. They modeled the channel as an independent Rayleigh fading channel and path loss with an arbitrary path loss exponent. However, they only considered multi-path or small-scale fading.

In [19] the authors studied the simulation part of large number of papers and found that most of the assumptions are overly simplistic and far from real network scenario. The authors then give general guidelines for the best simulation model of wireless networks. According to their experiments the best channel model is the one which consider both small-scale as well as large-scale (shadow) fading. Their experimental and simulation results were close enough when they considered both small-scale and large-scale fading.

2.2 Sum Distribution of Log-normal and Suzuki RVs

We consider two different channel models, i.e., shadowing and composite shadowing-fading. Shadowing is modeled as log-normal RV, because the received signal level at a specific transmitter-receiver separation follow Gaussian (normal) distribution, where all the measurement are in dB unit [21]. The composite envelope distribution is required when both shadowing and multipath are considered. In order to generate composite envelope, shadowing and fading process are generated separately and then multiplied together [20]. Composite shadowing-fading is modeled as Suzuki (Rayleigh-lognormal) RV. We know that in cooperative communication the received power on a single node is actually the sum of finite transmitted power from previous level node. In shadowing channel the received power is the sum of multiple log-normal RVs, while in composite channel it is the sum of multiple Suzuki RVs. However, there is no closed-form expression for the probability distribution function (PDF) of the sum of log-normal as well as Suzuki RVs. Therefore,

different approximation techniques are used to approximate the PDF of the sum of multiple log-normal and Suzuki RVs in closed-form.

Fenton and Wilkinson in [24] discussed the problem that what would be the distribution of sum of log-normal random variables. They approximated the sum of multiple log-normal RVs by another log-normal RV. The mean and standard deviation of the sum variable is found by matching the first two moments of sum variable to that of individual log-normal RVs. One major issue with Fenton-Wilkinson's method is that it breaks down at the higher dB spread of standard deviation. Schwartz and Yeh in [30] examined the problem of computing the distribution of a sum of independent log-normal RVs. They also approximated the sum by another log-normal RV. They derived exact expression for the first two moment of the sum of log-normal RVs. This method used a recursive approach and can only work for independent log-normal random variables. However later it was extended to correlated log-normal random variables. As compared to Fenton-Wilkinson's method this is much more complex.

Another approximation method known as Farley's approximation, also calculate the PDF of the sum of independent log-normal RVs by another log-normal RV [29]. Farley's estimate is actually a strict lower bound on the cumulative distribution function (CDF). Farley's estimate gives good result for large dB spread only. In [29] the authors compared these three methods, which are used to calculate the PDF of the sum of correlated log-normal RVs. They found that Fenton-Wilkinson's approach is the best method to compute the complementary distribution function of the sums of correlated log-normal RVs and hence the outage probability in correlated log-normal

shadowed mobile environments. This is due to both its accuracy and computational simplicity over the range of parameters valid for practical applications. Therefore, we use Fenton-Wilkinson method to find the PDF of the sum of multiple correlated log-normal RVs.

Similarly, to find the sum distribution of multiple Suzuki RVs different approximation techniques have been proposed in literature. In [23], a technique based on an extension of Fenton-Wilkinson's [24] approach is proposed. It is a two step approximation process, which approximates a Suzuki RV to a log-normal RV in the first step and then uses the Fenton-Wilkinson's method to find the sum distribution of the multiple log-normal RVs to a single log-normal RV. In [25], the sum of Suzuki RVs is approximated by a single Suzuki RV. However, this methods does not consider the problem of addressing the sum by a single log-normal RV. We use a more accurate method proposed in [26] to approximate the sum of Suzuki RVs by a single log-normal RV. This method uses moment generating function (MGF) as a tool to approximate the sum distribution. This method requires that both the MGF of log-normal and Suzuki RVs are to be in closed-form, neither of which exist in closed-form. Therefore, it uses the Gauss-Hermite [27] expansion of the MGFs of both log-normal and Suzuki to find the closed-form expression for it.

Since, cooperative communication for sensor network is a popular research area and its performance under the shadowing and composite shadowing-fading is not studied yet, this thesis provides a comprehensive analysis of linear cooperative multi-hop networks under the aforementioned channel models.

Chapter 3

Modeling by Markov Chain

In this chapter, we discuss the network model and the assumptions we made. We consider a one-dimensional network of equally-spaced nodes, where a group of nodes transmit cooperatively to another group of nodes. The transmission from one level to another is modeled as a discrete-time quasi-stationary Markov process. We also describe the insights given by the Perron-Frobenius eigenvalue of the transition probability matrix of the Markov chain. In Section 3.1, we describe our network parameters, while in Section 3.2, we model the network as a Markov process.

3.1 System Description

Consider a linear network with infinite number of nodes where the distance between the adjacent nodes is d, as shown in Fig. 3.1. The network is partitioned into non-overlapping groups of nodes, such that each group or *level* consists of M number of nodes. The nodes of a level cooperate with each other to send the same message signal to the next level. However, only

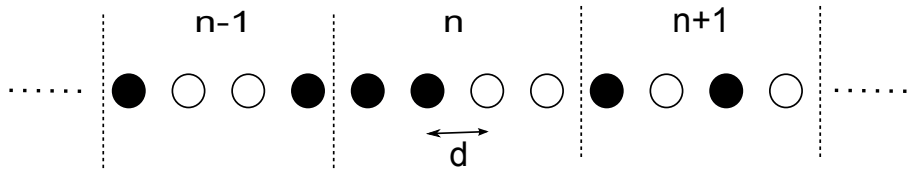

Figure 3.1: System model; $M = 4$.

those nodes take part in transmission, who have decoded the data perfectly from the transmission of previous level nodes. These nodes are known as decode-and-forward (DF) nodes. Diversity in this network can be achieved by employing frequency diversity, where each radio is assigned an orthogonal frequency, or by using appropriate space-time code. Besides the partition constraint, this network is still opportunistic in the sense that the number of nodes that decode the message in a level is unknown apriori. At any level, a node becomes DF, when the signal-to-noise ratio (SNR) of the received signal at that node after post-detection combining is greater than or equal to a modulation dependent threshold, τ. The filled circles in Fig. 3.1. show the DF nodes. We assume that the transmit power, P_t, is same for all nodes. We define $\mathbb{N}_n$ to be the set of indices of those nodes that decoded the message successfully at time instant or level n. For instance, from Fig. 3.1, $\mathbb{N}_{n-1} = \{1, 4\}$, $\mathbb{N}_n = \{1, 2\}$, and $\mathbb{N}_{n+1} = \{1, 3\}$. The received power at any time instant n on the kth node is given by

$$Pr_k(n) = \frac{P_t}{d^\beta} \sum_{m \in \mathbb{N}_{n-1}} \frac{\nu_{mk}}{(M - m + k)^\beta}, \tag{3.1}$$

where the summation is over the DF nodes in the previous level $(n-1)$ and β is the path loss exponent with a usual range of 2-4. The channel coefficient, ν_{mk}, is a log-normal RV, if we considered the channel as shadowing channel, and a Suzuki RV if the channel exhibits composite shadowing-fading. We

assume perfect synchronization between nodes of a level such that the DF nodes transmit the signal at the same time.

3.2 Modeling By Markov Chain

We represent the state of each node by a binary indicator RV, $\mathbb{I}$, such that at a time instant n the state of the kth node, $\mathbb{I}_k(n) = 1$ represents that node k has decoded successfully and $\mathbb{I}_k(n) = 0$ shows that node k has not decoded the data correctly. In the same way, the state of each level can be represented as $\mathcal{X}(n) = [\mathbb{I}_1(n), \mathbb{I}_2(n), ..., \mathbb{I}_M(n)]$ where the outcome of $\mathcal{X}(n)$ is an M-bit binary word. Each outcome is a state, and there are 2^M total number of states, starting from 0 to $2^M - 1$ in decimal. If i_n represents the state at time instant n then from Fig. 3.1. $i_n = \{1100\}$ in binary, and $i_n = 12$ in decimal. It can be noticed that $\mathcal{X}$ is a memoryless Markov process because the state at any time depends upon the transmissions from the previous level only. Further investigation reveals that the Markov chain, $\mathcal{X}$, can reach an absorbing state at any point in time with some nonzero probability, terminating the process of transmission. At that time the state of Markov chain will be 0 (decimal) and will happen only when all the nodes in a level fail to decode the message perfectly. Thus $\{0\} \cup T$ constitute the state space of the Markov chain $\mathcal{X}$, where T is the finite transient irreducible state space; $T = \left\{1, 2, ..., 2^{M-1}\right\}$ and 0 being the absorbing state such that

$$\lim_{n\to\infty} \mathbb{P}\{\mathcal{X}(n) = 0\} \nearrow 1 \text{ a.s.} \tag{3.2}$$

The Markov chain, $\mathcal{X}$, can be completely characterized by finding the transition probability matrix, $\mathbf{P}$, corresponding to $\mathcal{X}$. If we remove the transitions

to and from the absorbing states the resulting $\mathbf{P}$ is square, irreducible and right sub-stochastic with a dimension of $(2^M - 1) \times (2^M - 1)$ [32].

By the theory of Markov chain, a distribution $\mathbf{u} = (u_i, i \in T)$ is called ρ-invariant distribution if $\mathbf{u}$ is the left eigenvector of this particular transition matrix, $\mathbf{P}$, which corresponds to ρ, where ρ is the maximum eigenvalue of $\mathbf{P}$, i.e., $\mathbf{uP} = \rho\mathbf{u}$. In the meantime $\forall n, \mathbb{P}\{\mathcal{X}(n) = 0\} > 0$, therefore ultimate killing is certain. However, we are interested in finding the distribution of the transient states, just before the absorbing state is reached. This limiting distribution is known as the quasi-stationary distribution of the Markov chain [32], and is independent of the initial conditions of the process. The ρ-invariant distribution for one-step transition probability matrix of the Markov chain on T give us this unique distribution. To find the quasi-stationary distribution, we first calculate the *maximum* eigenvector, $\hat{\mathbf{u}}$, of $\mathbf{P}$. Defining $\mathbf{u} = \hat{\mathbf{u}} / \sum_{i=1}^{2^M-1} \hat{\mathbf{u}}_i$, as a normalized version of $\hat{\mathbf{u}}$ that sums to one gives the quasi-stationary distribution of $\mathcal{X}$. Hence the unconditional probability of being in state j at time instant n is given as

$$\mathbb{P}\{\mathcal{X}(n) = j\} = \rho^n u_j, \ j \in T, n \geq 0. \tag{3.3}$$

We also let $\Phi = \inf\{n \geq 0 : \mathcal{X}(n) = 0\}$ denotes the end of survival time, i.e., the time at which the killing occurs. It follows then

$$\mathbb{P}\{\Phi > n + n_0 | \Phi > n\} = \rho^{n_0}, \tag{3.4}$$

while the quasi-stationary distribution of the Markov chain is given as

$$\lim_{n\to\infty} \mathbb{P}\{\mathcal{X}(n) = j | \Phi > n\} = u_j, \ j \in T. \tag{3.5}$$

Chapter 4

Model for Shadowing

In this chapter, we consider the shadowing channel and derive the transition probability matrix of the Markov chain, which depends upon the underlying distribution of the received power. The received power is modeled as a log-normal RV and its distribution is derived by using Fenton-Wilkinson's approximation technique. The eigen-decomposition of the transition probability matrix provides insightful information about the network coverage and various other parameters. We quantify the values of the signal-to-noise ratio (SNR) margin required to get a desired coverage distance under a given quality-of-service (QoS) and standard deviation of shadowing constraints. We use numerical simulations to check the accuracy of our analytical model. In Section 4.1, we describe log-normal shadowing.

In Section 4.2, we obtain the sum distribution of the log-normal RVs and find the transition probability matrix of the Markov chain. In Section 4.3, we discuss the results and network performance.

4.1 Log-normal Shadowing

The fluctuations in the received power of the wireless channel is due to the combined effect of the two fading processes; the small-scale fading and the large-scale fading, also known as shadowing. The small-scale fading or multi-path fading is due to the existence of multiple paths between the transmitter and receiver. The signals from these multiple paths either interfere constructively or destructively at the receiver. Shadowing occur when the path between the transmitter and the receiver is obstructed by surface that has sharp irregularities (edges). The fluctuations in the received power due to shadowing is experienced on the local-mean power [21]. In this chapter, we study shadowing for the network model of the Fig. 3.1. Since, we are considering the shadowing channel and shadowing is modeled as log-normal RV then the channel coefficient ν_{mk}, in (3.1) is a log-normal RV. The PDF of a log-normal RV, ν, is given as

$$p(\nu) = \frac{1}{\sqrt{2\pi}\sigma\nu} \exp - \left(\frac{(\ln \nu - \mu)^2}{2\sigma^2} \right). \tag{4.1}$$

The log-normal RV, $\nu = e^Y$, where $Y \sim \mathcal{N}(\bar{\mu}, \bar{\sigma}^2)$; $\bar{\mu} = \lambda\mu$ and $\bar{\sigma}^2 = \lambda\sigma^2$, where μ (dB) is the mean of ν, σ_Y (dB) is the standard deviation of Y, and $\lambda = \ln 10/10$ [29]. The standard deviation, σ, is called the dB spread and its typical value is between 5-12 dB for practical channels, depending upon the severity of the shadowing.

4.2 Formulation of Transition Probability Matrix for Shadowing Channel

Here, we find the state transition probability matrix, $\mathbf{P}$, for our model, the eigenvector of which is quasi-stationary distribution. Let i and j denote a pair of states of the system at time instant $(n-1)$ and n, respectively, such that $i,\ j \in \left\{1, 2, ..., 2^M - 1\right\}$, where i and j are the decimal equivalent of the binary word formed by the set of indicator RVs. Let the received SNR at the kth node at time instant n be $\gamma_k(n) = Pr_k(n)/\sigma^2_{noise}$, where σ^2_{noise} is the variance of noise at kth receiver, and Pr is the received power as given in (3.1). Without the loss of generality, we assume identical noise variances for all the nodes at any time instant. Now for each node k, the conditional probability of being able to decode at time n is given as

$$\begin{aligned} &\mathbb{P}\left\{\text{node } k \text{ of level } n \text{ will decode } |\psi\right\} = \\ &\mathbb{P}\left\{\mathbb{I}_k(n) = 1|\psi\right\} = \mathbb{P}\left\{\gamma_k(n) > \tau|\psi\right\}, \end{aligned} \tag{4.2}$$

where the event ψ is defined as $\psi = \{\mathcal{X}(n-1) \in S\}$, implying that the previous state is a transient state. In the same way, the probability of outage or the probability of $\mathbb{I}_k(n) = 0$ is given as $1 - \mathbb{P}\left\{\gamma_k(n) > \tau|\psi\right\}$, where

$$\mathbb{P}\left\{\gamma_k(n) \geq \tau|\psi\right\} = \int_{\tau}^{\infty} p_{\gamma_{k|\psi}}(y)dy, \tag{4.3}$$

where $p_{\gamma_{k|\psi}}$ is the conditional PDF of the received SNR at the kth node conditioned on the state $\mathcal{X}(n-1)$. It can be noted that the received power at a certain node is the sum of the finite powers from the previous level nodes, each of which is log-normally distributed. However, the sum of log-normal RVs does not have a closed form expression [20]. Therefore, we

use Fenton-Wilkinson's approximation method to find the sum distribution [24]. This method was originally developed for independent log-normal RVs, but it was extended for the approximation of correlated log-normal RVs in [29]. We want to find the complementary distribution function of the sum of N correlated log-normal RVs $(\gamma_1, \gamma_2, ..., \gamma_N)$, where $\max|N| \leq M$. Let $\gamma = \gamma_1 + \gamma_2 + ... + \gamma_N$. This method approximates the sum of log-normal RVs by another log-normal RV. So γ becomes

$$\gamma = e^{Y_1} + e^{Y_2} + ... + e^{Y_N} \cong e^L, \tag{4.4}$$

where L is a Gaussian RV; $L = \sum_{m=1}^{N} Y_m$, and each Y_m is also Gaussian RV with mean μ_{Y_m} and variance $\sigma^2_{Y_m}$. To create a vector of N correlated Gaussian RVs $\mathbf{Y} = [Y_1, Y_2, ..., Y_N]^T$, where T denotes the transpose operation, first a vector of uncorrelated Gaussian RV, $\mathbf{X}$, is created. Then by using a linear transformation $\mathbf{Y} = \mathbf{CX}$, the desired correlated RVs are obtained. The matrix $\mathbf{C}$ is given as $\mathbf{\Gamma} = \mathbf{CC}^T$, and is found by using the Cholesky factorization [36], where $\mathbf{\Gamma}$ is the correlation matrix given by

$$\mathbf{\Gamma} = \begin{bmatrix} 1 & r_{12} & \cdots & r_{1N} \\ r_{21} & 1 & \cdots & r_{2N} \\ \vdots & \vdots & \ddots & \vdots \\ r_{N1} & r_{N2} & \cdots & 1 \end{bmatrix}.$$

$\mathbf{\Gamma}$ is symmetric and positive semi-definite, which is a necessary condition for correlation model [34]. It is important to mention that the size of $\mathbf{\Gamma}$ may change on every hop as the number of DF nodes may change from level to level. Remember that each X_m denotes the received SNR when mth node in the previous level transmits. We select identical variance σ^2 for each X_m,

however, because of the path loss the mean of each X_m varies and is given as

$$\mu_{X_m} = \frac{P_t}{d^{\beta}\left(M-m+k\right)^{\beta}}, \tag{4.5}$$

where k is the position of the receiving node at time instant n, m is the position of the transmitting node at level $(n-1)$, and the rest of the variables have the usual meaning.

The mean ${\mu_L}^{(k)}$ and standard deviation ${\sigma_L}^{(k)}$ of L at kth node in (4.4) in Fenton-Wilkinson's method is found by matching the first two moments of L with the first two moments of $(\gamma_1+\gamma_2+...+\gamma_N)$. Let ϕ_1 and ϕ_2 represent the first and second moment of $(\gamma_1+\gamma_2+...+\gamma_N)$, respectively, then matching the first moment gives

$$\mathbb{E}\left[\gamma\right] = e^{{\mu_L}^{(k)}+{\sigma_L^2}^{(k)}/2} = \sum_{m=1}^{N} e^{\mu_{Y_m}+\sigma^2_{Y_m}/2} = \phi_1. \tag{4.6}$$

In the same way, matching the second moment gives

$$\mathbb{E}\left[\gamma^2\right] = e^{2{\mu_L}^{(k)}+2{\sigma_L^2}^{(k)}} = \sum_{m=1}^{N} e^{2\mu_{Y_m}+2\sigma^2_{Y_m}} + 2\sum_{m=1}^{N-1} \sum_{l=m+1}^{N} \left\{ e^{\mu_{Y_m}+\mu_{Y_l}} e^{\frac{1}{2}\left(\sigma^2_{Y_m}+\sigma^2_{Y_l}+2r_{ml}\sigma_{Y_m}\sigma_{Y_l}\right)} \right\} = \phi_2, \tag{4.7}$$

where r_{ml} is the correlation coefficient between Y_m and Y_l. From (4.6) and (4.7) the ${\mu_L}^{(k)}$ and ${\sigma_L^2}^{(k)}$ can be obtained as

$${\mu_L}^{(k)} = 2\ln\phi_1 - \frac{1}{2}\ln\phi_2, \tag{4.8}$$

$${\sigma_L^2}^{(k)} = \ln\phi_2 - 2\ln\phi_1. \tag{4.9}$$

Hence the conditional probability of a single node, k, to decode correctly in (4.3) becomes

$$\mathbb{P}\left\{\gamma^{(k)} \geq \tau|\psi\right\} = \mathbb{P}\left(e^L \geq \tau\right) = \mathbb{P}\left(L \geq \ln\tau\right) = Q\left(\frac{\ln\tau - {\mu_L}^{(k)}}{{\sigma_L}^{(k)}}\right), \tag{4.10}$$

where $\gamma^{(k)}$ is the received SNR at kth node in the receiving level at time instant n, ${\mu_L}^{(k)}$ and ${\sigma_L}^{(k)}$ denote the mean and standard deviation of the SNR at node k, where $k = \{1, 2, ..., M\}$ and the respective SNR levels of other nodes change by (4.8) and (4.9), which are further dependent upon (4.5) and the number of transmitting nodes N. In (4.10), Q-function denotes the tail probability; $Q(x) = \frac{1}{2\pi}\int_x^\infty e^{-t^2/2}dt$. Equation (4.10) describes the success probability of one node. For M nodes in a level, let $\mathbb{N}_n^{(j)}$ and $\overline{\mathbb{N}}_n^{(j)}$ denote the set of indices of those nodes, which are 1 and 0, respectively, at time instant n in state j, then the one-step transition probability for going from state i to j is given as

$$\mathbb{P}_{ij} = \prod_{k\in\mathbb{N}_n^{(j)}} \left\{ Q\left(\frac{\ln\tau - {\mu_L}^{(k)}}{{\sigma_L}^{(k)}}\right)\right\} \times \prod_{k\in\overline{\mathbb{N}}_n^{(j)}} \left\{ 1 - Q\left(\frac{\ln\tau - {\mu_L}^{(k)}}{{\sigma_L}^{(k)}}\right)\right\}. \quad (4.11)$$

Equation (4.11) provides one entry of the matrix $\mathbf{P}$. Similar procedure is used to find all the entries of $\mathbf{P}$, which can then be used to find the quasi-stationary distribution of the Markov chain.

4.3 Results and Performance Analysis of Shadowing Model

In this section, we present numerical results based on simulation and analysis. Various correlation models have been proposed in literature, however, we use an exponential model to characterize the correlation between the channel gains of various transmitters. More specifically, the correlation between transmitters decorrelates exponentially with distance [34]. The correlation coefficient between two transmitters x and y is given as $r_{xy} = \exp^{-|d_{xy}|/d_0}$,

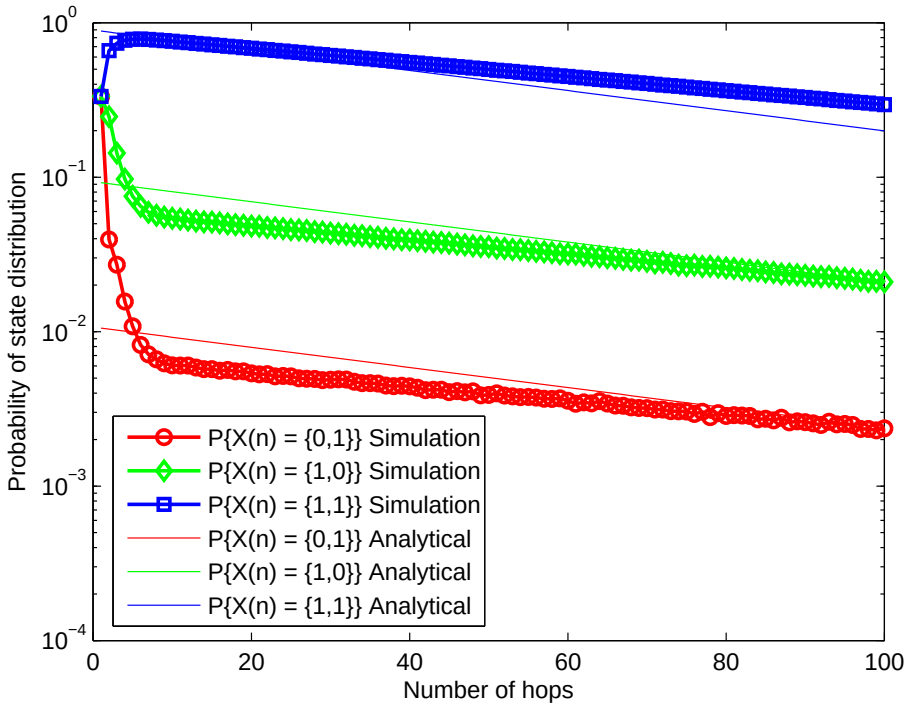

Figure 4.1: Comparison of state distribution of analytical and simulation model; for $M = 2$.

where d_{xy} is the distance between x and y and d_0 is a tunable parameter called the decorrelation distance. Without the loss of generality, we assume $d_0 = 1$ throughout our results. For simulation purposes, we calculate the received power at each node based on the previous state (assuming an initial distribution for the first hop), which sets the indicator functions as either 0 or 1 depending upon the threshold criterion. These indicator functions form the current state and the process continues until an absorbing state is reached. We obtain the distribution of the chain by averaging over 1 million simulation trials.

Fig. 4.1. shows the probability of state distribution of the Markov chain

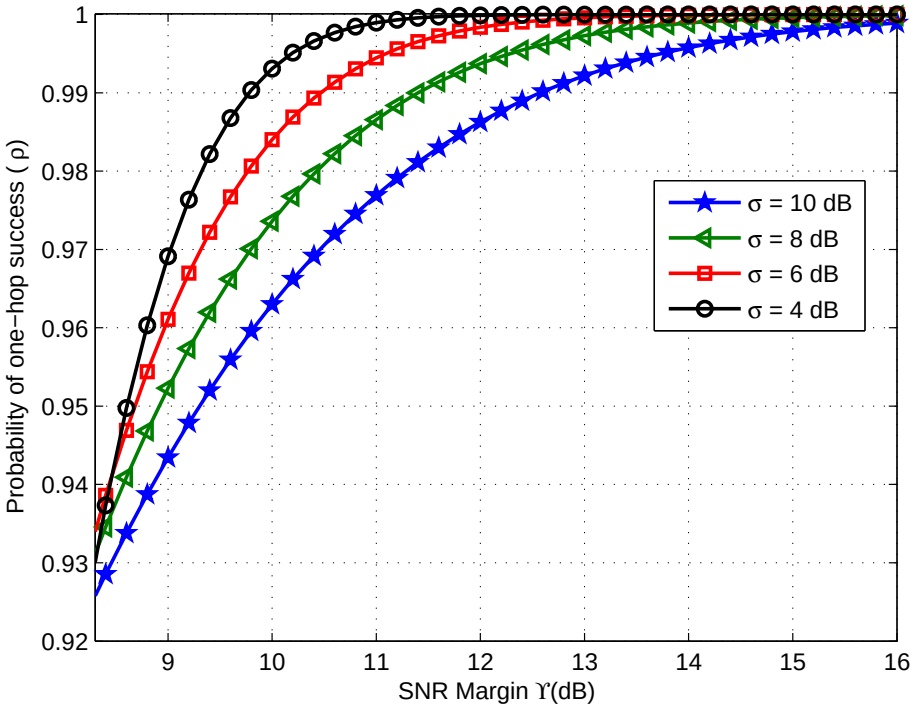

Figure 4.2: Probability of one-hop success vs. SNR margin for $M = 3$.

at different hops, for $M = 2$, $r_{xy} = 0.3$, and $\sigma = 4$dB. In this case, the total number of transient states are 3, namely $\{0, 1\}$, $\{1, 0\}$, and $\{1, 1\}$. The figure shows the probability of being in all three states at various hops by using both the network simulation results and the analytical model. It can be seen that analytical results are quite close to simulation results, which shows the validity of our analytical model. It can be noticed that as the hop count increases, the probability of being in transient state decreases, which shows that eventually the transmission will stop propagating. Similar results are obtained for other values of M, which are not shown here to avoid repetition. The rest of the figures, i.e., Figs. 4.2-4.4 are based on analytical model.

Fig. 4.2. shows the probability of one-hop success, ρ, which is the prob-

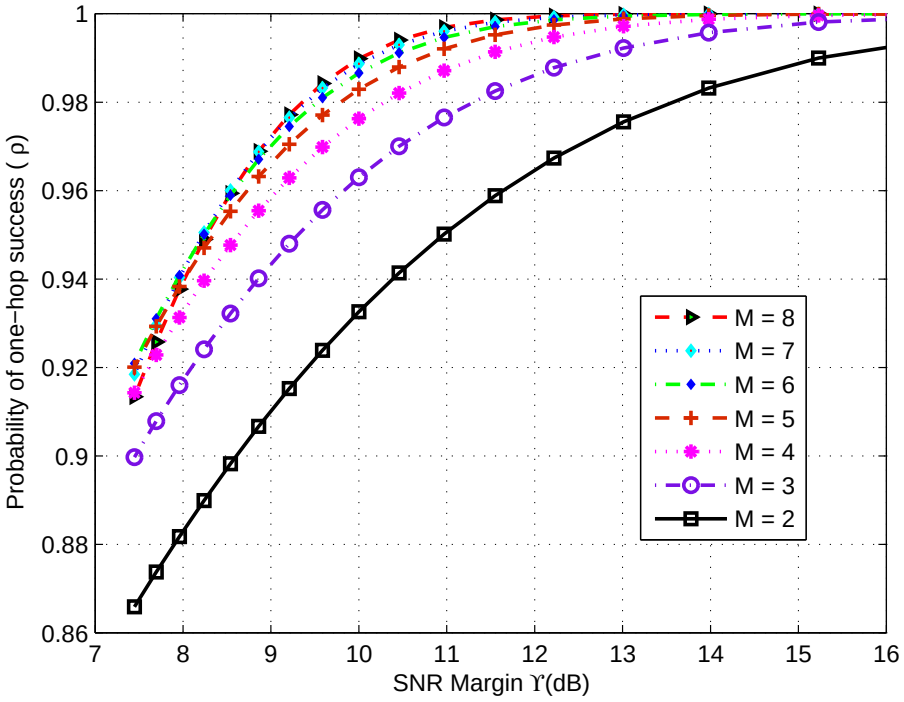

Figure 4.3: Probability of one-hop success vs. SNR margin for $\sigma = 10$dB.

ability that at least one node in a level decoded successfully, versus SNR margin, Υ, for various values of shadowing standard deviation, σ, and keeping $M = 3$ fixed. One-hop success probability is given by the maximum eigenvalue of $\mathbf{P}$ and SNR margin, Υ, is defined by normalizing the received SNR at a node, which is a distance d away from its transmitter. Specifically, $\Upsilon = \frac{P_t}{d^\beta \tau}$. For the simulation results, we keep unit P_t and unit d, while $\beta = 2$. It can be noticed that as the SNR margin is increased, the one-hop success probability also increases. However, by increasing the standard deviation, σ, of log-normal shadowing for a fixed value of Υ, the probability of success drops, which shows the effect of the severity of shadowing on the network performance. All curves for various σ converge at higher Υ, which shows

that by increasing Υ we can overcome the loss incurred by shadowing.

In Fig. 4.3. by keeping the σ constant, we plot the probability of one-hop success, ρ, against Υ for various values of M. It can be seen that by increasing M, the probability of success also increases, which shows the effect of increased transmitter diversity on the system. For a fixed Υ, if we define the gain in success probability as, $\Delta\rho_{xy} = \rho|_{M=y} - \rho|_{M=x}$, then it can be seen that $\Delta\rho_{23}$ is larger as compared to $\Delta\rho_{34}$. For example at Υ of 8 dB, $\Delta\rho_{23} \approx 0.036$ while $\Delta\rho_{34} \approx 0.01$. Thus it shows that the diversity gain obtained while increasing M has a *diminishing* behavior and once reached to saturation, a further increase in M will not achieve any gain at a particular value of Υ.

From the deployment perspective of the network, it is some times required to optimize the values of certain parameters like transmit power of relays or distance between them. This optimization is done to obtain a certain quality of service (QoS), η. The QoS is the probability of delivering the message to a certain distance without being entered into the absorbing state, and the ideal value of η is 1. Thus the theory of quasi-stationary Markov chain [32] provides an upper bound on the number of hops, n_0, one can go with a given η, i.e., $\rho^{n_0} \geq \eta$, which gives $n_0 \leq \frac{\ln \eta}{\ln \rho}$. Multiplying the number of hops, n_0, by M provides the maximum distance that can be reached with a certain QoS, η. Fig. 4.4. shows the contours of normalized distance that can be reached as a function of η and σ, at a specific SNR margin of $\Upsilon = 15$ dB and $M = 6$. We normalize the distance by dividing it by the maximum distance, which for this particular case is $1.8167e8$. Normalization is only done for a better representation of the figure. It can be noticed that a particular coverage

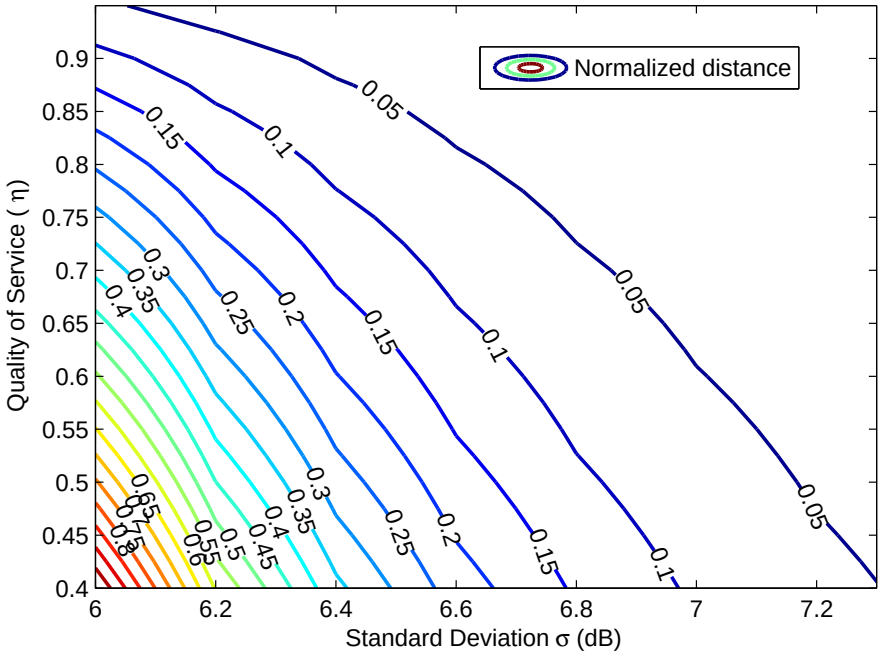

Figure 4.4: Contours of normalized distance as a function of η and σ; $\Upsilon = 15$ dB and $M = 6$.

can be obtained by having different combinations of η and σ. However, σ is environment dependent and by keeping all other parameters such as Υ and M fixed, the message can only reach larger distance with low QoS. Further, it can be noted from the figure that σ severely effects QoS. For example a normalized distance of 0.1 can be reached with $\eta \approx 0.9$ when $\sigma \approx 6$ dB, however, when $\sigma \approx 7$ dB, then the same normalized distance of 0.1 can be reached with $\eta \approx 0.4$, reflecting a loss in QoS.

Comparing the result of Fig. 4.4. in this chapter for shadowing, to that of Fig. 6. of small-scale fading in [18], provides an insight that both shadowing and fading have nearly similar effects on the performance of the network under consideration for specific value of σ. For example, if we compare the

coverage distance under shadowing for $\sigma = 6$ dB to that of small-scale fading, while keeping all other parameters same, i.e., $M = 6, \eta = 0.9, \Upsilon = 15$ dB, and $\beta = 2$, we interestingly find that approximately same distance can be reached by both channel models. However, if we increase σ of shadowing, then it is clear from Fig. 4.4. that the coverage distance reduces drastically and we get a normalized coverage distance of ≈ 0.05 at $\sigma = 6.5$ dB, which is half as compared to ≈ 0.1 at $\sigma = 6$ dB. This finding indicates that one must consider both small-scale as well as large-scale fading for the system under consideration.

Chapter 5

Model for Composite Shadowing-Fading

In this chapter, we derive the transition probability matrix of the Markov chain by considering the wireless channel exhibiting composite shadowing-fading. The multipath fading is modeled as Rayleigh RV and shadowing as a log-normal RV, the mixture distribution is known as Suzuki (Rayleigh-lognormal) RV. The sum distribution of the multiple Suzuki RVs is approximated to a single log-normal RV by using the moment generating function (MGF)-based technique. This MGF-based technique uses Gauss-Hermite integration to present the sum distribution in closed form. We quantify the SNR margin required to achieve a certain QoS under standard deviation of the shadowing. We also provide the optimal level of cooperation required for obtaining maximum coverage of a line network under a given QoS. Two topologies for linear network are considered and the performance of each topology under various system parameters is provided. The analytical results are validated through simulation results.

Section 5.1 describes composite shadowing-fading. In Section 5.2, we derive the transition probability matrix of the Markov process. In Section 5.3, we validate our analytical model through simulation results, and discuss our results and system performance.

5.1 Composite Shadowing-Fading

A wireless channel exhibits composite shadowing-fading when both multipath fading and shadowing are present. In composite channel model the received power at a node, while using the same network model of Fig. 3.1. is given by,

$$Pr_k(n) = \frac{P_t}{d^\beta} \sum_{m \in \mathbb{N}_{n-1}} \frac{S_{mk}}{(M-m+k)^\beta}, \tag{5.1}$$

where, S_{mk} is the composite channel coefficient, from node m in level $(n-1)$ to node k in level n, while the rest of the parameters have the same meaning as in Chapter 3. We model the composite channel as a Suzuki RV, which is a combination of Rayleigh and log-normal RVs. We use Rayleigh distribution for the multipath fading and log-normal distribution for the shadowing. The PDF of the Suzuki distribution is given by

$$p(s) = \int_0^\infty \frac{s}{w^2} \exp\left(-\frac{s^2}{2w^2}\right) \frac{1}{\sqrt{2\pi}w\sigma} \exp\left(-\frac{(\log w - \mu)^2}{2\sigma^2}\right) dw, \tag{5.2}$$

where w is the Rayleigh parameter and μ and σ^2 are the mean and variance of the log-normal RV [22]. Both μ and σ are expressed in decibel. The standard deviation, σ, is the dB spread of the channel and its typical value is between 5-12 dB for wireless channels depending upon the severity of the shadowing.

5.2 Formulation of Transition Probability Matrix for Composite Shadowing-Fading Channel

In this section, we find the state transition probability matrix, $\mathbf{P}$, of the network, by considering the channel as composite fading channel. Let i and j represent the two states of the system at time instant $(n-1)$ and n, respectively, such that $i,\ j \in \left\{1, 2, ..., 2^M - 1\right\}$, where i and j are the decimal equivalent of the binary word formed by the set of binary indicator RVs. The received SNR at time instant n on the kth node is given as $\gamma_k(n) = Pr_k(n)/\sigma^2_{noise}$, where σ^2_{noise} is the noise variance at the kth receiver, and Pr is the received power as given in (5.1). For all the nodes in a level we assume identical noise. Now for a node k, the conditional probability of being able to decode successfully at time n is given as

$$\mathbb{P}\left\{\text{node } k \text{ of level } n \text{ will decode } |\varphi\right\} = \mathbb{P}\left\{\mathbb{I}_k(n) = 1|\varphi\right\} = \mathbb{P}\left\{\gamma_k(n) > \tau|\varphi\right\}, \tag{5.3}$$

where the event φ is defined as $\varphi = \{\mathcal{X}(n-1) \in S\}$, indicating that the previous state is a transient state. Similarly, the probability of outage or the probability of $\mathbb{I}_k(n) = 0$ is given as $1 - \mathbb{P}\left\{\gamma_k(n) > \tau|\varphi\right\}$, where

$$\mathbb{P}\left\{\gamma_k(n) \geq \tau|\varphi\right\} = \int_{\tau}^{\infty} p_{\gamma_{k|\varphi}}(y)dy, \tag{5.4}$$

where $p_{\gamma_{k|\varphi}}$ is the conditional PDF of the received SNR at the kth node conditioned on the state $\mathcal{X}(n-1)$. It can be observed that the received SNR at a certain node is the sum of the finite SNRs from the previous level nodes[1],

[1]assuming maximal ratio combining for coherent modulation scheme

each of which follow Suzuki (Rayleigh-lognormal) distribution. However, the distribution of the sum of Suzuki RVs does not exist in closed-form [20]. Therefore, to find the sum distribution of Suzuki RVs, we use the moment generating function (MGF)-based technique as proposed in [26]. The MGF of a RV, Y is given by

$$\Psi_Y(s) = \int_0^\infty \exp(-sy) p_Y(y) dy. \tag{5.5}$$

MGF exhibits two important properties; first, MGF is the weighted integral of the PDF with adjustable parameter s and second, the MGF of the sum of independent RVs can be expressed as the product of the MGFs of individual RVs as given by

$$\Psi_{(\sum_{k=1}^{N} Y_k)}(s) = \prod_{k=1}^{N} \Psi_{Y\,k}(s). \tag{5.6}$$

We approximate the sum of N Suzuki RVs $(S_1, S_2, ..., S_N)$ by a single log-normal RV, $Y = 10^{0.1X}$, where X is a Gaussian RV. This MGF-based approximation method requires that both the MGF of Suzuki and log-normal RV need to be in closed-form. However, the MGF of both the Suzuki and log-normal RV does not exist in closed-form and can be numerically computed using the Gauss-Hermite quadrature integration [27]. In Gauss-Hermite quadrature integration, the integral is evaluated by an approximate sum where each component of the summation depends upon a specific weight. Specifically the MGF of kth Suzuki RV by Gauss-Hermite integration after discarding the remainder terms can be written as

$$\widehat{\Psi}_{S_k}(s; \mu_k, \sigma_k) = \sum_{c=1}^{C} \frac{w_c/\sqrt{\pi}}{1 + s \exp\left(\frac{\sqrt{2}\sigma_k a_c + \mu_k}{\xi}\right)}, \tag{5.7}$$

where C is the Hermite integration order and a large value of C corresponds to higher accuracy, w_c is the weight corresponding to the abscissas, a_c, and

ξ is a constant; $\xi = 10/\ln 10$. The values of w_c and a_c for C up to 20 are available in tabular form in [28]. The μ_k and σ_k are the mean and standard deviation of the kth Suzuki RV. Hence the MGF of the sum of N Suzuki RVs $(S_1, S_2, ..., S_N)$ is given as

$$\widehat{\Psi}_{(S_1+S_2+...+S_N)} = \prod_{k=1}^{N} \widehat{\Psi}_{Sk}(s; \mu_k, \sigma_k), \tag{5.8}$$

where each $\widehat{\Psi}_{Sk}$ is given in 5.7. Similarly, by using the Gauss-Hermite integration, the MGF of the log-normal RV, $Y = 10^{0.1X}$ is given as

$$\widehat{\Psi}_Y(s; \mu_X, \sigma_X) = \sum_{c=1}^{C} \frac{w_c}{\sqrt{\pi}} \exp\left[-s \exp\left(\frac{\sqrt{2}\sigma_X a_c + \mu_X}{\xi}\right)\right], \tag{5.9}$$

where μ_X and σ_X are the mean and standard deviation of the Gaussian RV X. The task is to find the μ_X and σ_X of X as a function of the mean and standard deviation of the individual RVs $(S_1, S_2, ..., S_N)$. The μ_X and σ_X can be found by solving the following two equations

$$\widehat{\Psi}_Y(s_i; \mu_X, \sigma_X) = \prod_{k=1}^{N} \widehat{\Psi}_{S_k}(s_i; \mu_k, \sigma_k), \text{ at } i = 1 \text{ and } 2. \tag{5.10}$$

By using 5.7 and 5.9, Equation 5.10 becomes

$$\sum_{c=1}^{C} \frac{w_c}{\sqrt{\pi}} \exp\left[-s_i \exp\left(\frac{\sqrt{2}\sigma_X a_c + \mu_X}{\xi}\right)\right] = \prod_{k=1}^{N} \left(\sum_{c=1}^{C} \frac{w_c/\sqrt{\pi}}{1 + s_i \exp\left(\frac{\sqrt{2}\sigma_k a_c + \mu_k}{\xi}\right)}\right), \text{ at } i = 1 \text{ and } 2, \tag{5.11}$$

where, as already stated μ_X and σ_X are the unknown. The right hand side of (5.11) consists entirely of known quantities and is evaluated twice at s_1 and s_2. By evaluating at $s_1 = 0.2$ we can find μ_X, while using $s_2 = 1.0$ gives σ_X. The values of s_1 and s_2 have been found by solving an optimization problem

as listed in [26]. It can be noted that (5.11) is a non linear equation and can only be solved numerically. We used `fsolve` function in MATLAB to solve it. Once the values of μ_X and σ_X have been calculated, the description of the sum distribution can be completely specified, i.e., the sum of Suzuki RVs has been approximated by a log-normal RV with calculated μ_X and σ_X. Hence the conditional probability that the received SNR ($Y^{(k)} = 10^{0.1X^{(k)}}$) at the kth node is greater than or equal to τ in 5.4 becomes

$$\mathbb{P}\left\{Y^{(k)} \geq \tau|\varphi\right\} = \mathbb{P}\left(10^{0.1X^{(k)}} \geq \tau\right) =$$
$$\mathbb{P}\left(X^{(k)} \geq 10\log\tau\right) = Q\left(\frac{10\log\tau - {\mu_X}^{(k)}}{{\sigma_X}^{(k)}}\right), \tag{5.12}$$

where Q-function denotes the tail probability; $Q(x) = \frac{1}{2\pi}\int_x^\infty e^{-t^2/2}dt$. Thus the success probability of a node depends upon the threshold τ, μ_X, and σ_X; while the μ_X and σ_X further depend on the number N of Suzuki RVs (the number of DF nodes) and the μ and σ of each Suzuki RV as given in (5.11). Equation (5.12) provides us the success probability of a single node to decode. For M nodes in a level, consider $\mathbb{N}_n^{(j)}$ and $\overline{\mathbb{N}}_n^{(j)}$ as the set of indices of those nodes, which are 1 and 0, respectively, at time instant n in state j, then the one-step transition probability of going from state i to state j is given by

$$\mathbb{P}_{ij} = \prod_{k\in\mathbb{N}_n^{(j)}}\left\{Q\left(\frac{10\log\tau - {\mu_X}^{(k)}}{{\sigma_X}^{(k)}}\right)\right\} \times$$
$$\prod_{k\in\overline{\mathbb{N}}_n^{(j)}}\left\{1 - Q\left(\frac{10\log\tau - {\mu_X}^{(k)}}{{\sigma_X}^{(k)}}\right)\right\}. \tag{5.13}$$

The one step transition probability is the product of the success probabilities of those nodes, which decode successfully, times the product of the outage probabilities of those nodes, which do not decode successfully. Equation

(5.13) gives one entry of the matrix $\mathbf{P}$. Similarly, we can find the transition probability matrix $\mathbf{P}$ by finding the transition probabilities for all the transient state space.

5.3 Results and Performance Analysis of Composite Channel

In this section, we present our simulation and analytical results. We obtain all the results by considering the composite channel model unless otherwise stated. In order to simulate the composite envelope, we generate the fading and shadowing processes separately and then multiply them together, while keeping unit mean for the fading envelope [20]. For simulation purposes, we first assume an initial distribution of the first hop and then calculate the received power at a node in the next hop. The indicator function $\mathbb{I}$ is set to 1 only if the received power is greater than the threshold τ. Same procedure is repeated for all the nodes in the current hop, which forms the current state and the process continues until an absorbing (all-zero) state is encountered. Fig. 5.1. shows the probability of state distribution of the Markov chain at different hops, for $\sigma = 10$ dB and $M = 2$. For $M = 2$, the total number of transient states are 3, namely $\{0, 1\}$, $\{1, 0\}$, and $\{1, 1\}$, and this figure shows the probability of being in these transient states at various hops by using both the simulation results and the analytical model. The simulation results are obtained by averaging over one million simulation experiments, whereas the analytical curves are obtained by using (3.3). It is clear from the figure that both the analytical and the simulation results are quite close to each

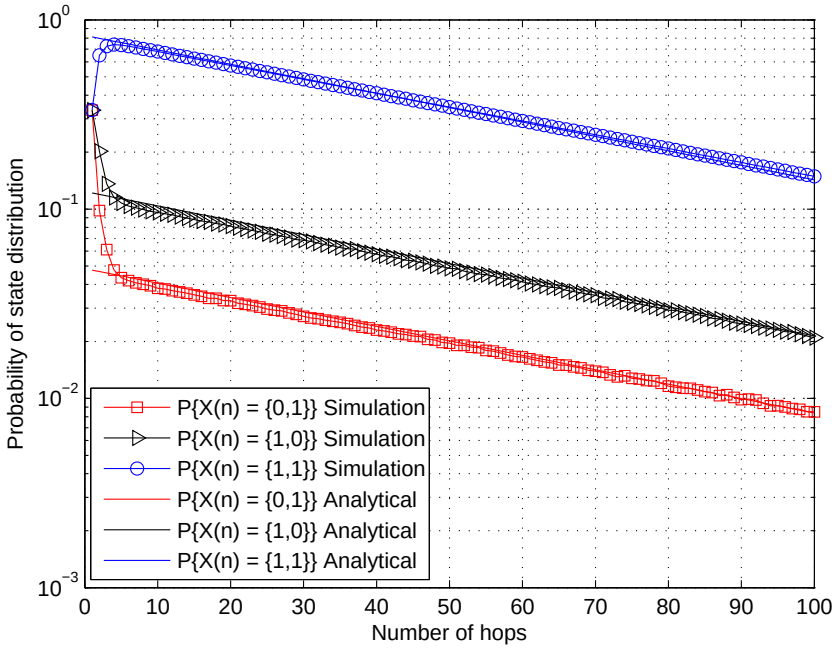

Figure 5.1: Comparison of analytical and simulation model for $M = 2$.

other, which confirms the accuracy of the proposed analytical model. It can be noticed for the simulation results that the initial distribution of all the three states have nearly equal probability of occurrence, i.e., 1/3. However, as the hop count increases, the distribution approaches the quasi-stationary distribution obtained from (3.3). The probability of being in a transient state decreases as the hop count increases, which shows that eventually the transmission will stop propagating, which is in accordance with Equation (3.2). It can be further observed that the slopes of the curves for all the three transient state remain the same, which means that the probability of being in either of these states remain unchanged regardless of the number of hops. Similar results are obtained for other M, which are not shown here to avoid repetitions.

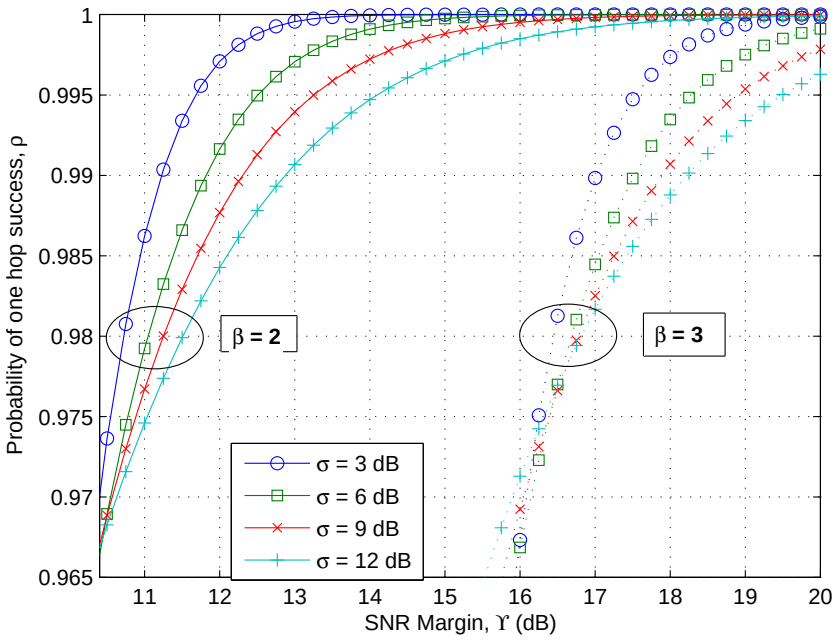

Figure 5.2: Probability of one-hop success vs. SNR margin for $M = 3$.

Before discussing further results, we define a few terms such as probability of one-hop success, ρ and the SNR margin, Υ. The probability of one-hop success, ρ, is the probability that at least one node in a level decodes successfully or, in other words, the probability that the Markov chain $\mathcal{X}(n)$ is in a transient state T, i.e., $\mathbb{P}\{\mathcal{X}(n) \in T\}$. This probability of one-hop success is given by the Perron-Frobenius eigenvalue of $\mathbf{P}$ [31]. The SNR margin, Υ, is the normalized received SNR at a node, which is a distance d away from it transmitter such that

$$\Upsilon = \frac{P_t}{d^{\beta}\tau}. \tag{5.14}$$

We assume unit P_t and unit d for all the results, while β and τ have their usual meaning of path loss exponent and the modulation dependent threshold, respectively. The value of β is 2 unless otherwise stated. Thus, if SNR

margin is 10 dB, then $P_t = 1$, $d = 1$, $\beta = 2$, and $\tau = 0.1$. In the same way we change the SNR margin by changing τ. For Fig. 5.2. and onwards all the results are obtained through the analytical model.

Fig. 5.2. shows the probability of one-hop success ρ, versus SNR margin Υ for different values of shadowing standard deviation σ and keeping $M = 3$ fixed. It can be noticed that for a specific σ, as the SNR margin is increased, the probability of one-hop success also increases. However, by increasing the σ of the log-normal shadowing, the probability of one-hop success drops at a specific value of SNR margin, which shows the effect of the severity of shadowing on the network performance. It can also be noticed that if we increase the path loss exponent, β, from 2 to 3 then an additional SNR margin of 6 dB (approximately) is required to achieve the same ρ. It can further be noticed that all the curves for different σ converge at higher Υ, which show that by increasing Υ we can overcome the losses incurred due to composite fading and path loss.

For the deployment point of view, it is desired to optimize certain parameters like transmit power of the nodes or the distance between them to achieve certain quality of service (QoS), η. The QoS is defined as the probability that a message is delivered to a certain distance without being entered into an absorbing state. The ideal value of QoS is 1. We can use (3.4) to find an upper bound on the number of hops, n_0, one can go with a given η, i.e., $\rho^{n_0} \geq \eta$, which gives

$$n_0 \leq \frac{\ln \eta}{\ln \rho}, \tag{5.15}$$

while by multiplying the number of hops n_0 by M gives the maximum distance than can be reached with a certain QoS η. Fig. 5.3. shows the contours

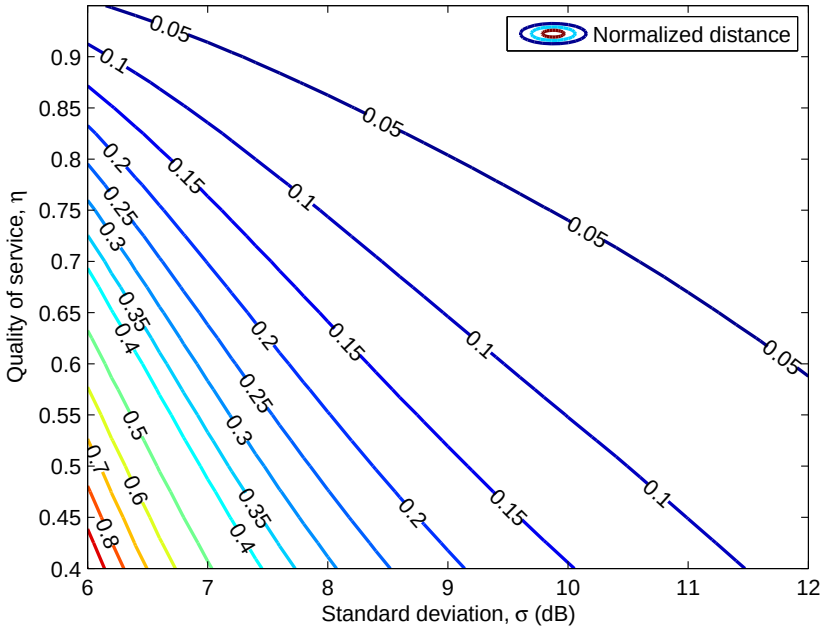

Figure 5.3: Contour of normalized distance as a function of η and σ; $\Upsilon = 15$ db and $M = 3$.

of the network coverage in term of normalized distance as a function of η and σ at a specific SNR margin of $\Upsilon = 15$ dB and $M = 3$. The normalization is done for a better representation of the figure. It can be noticed that a particular distance can be reached by different combination of η and σ. The increase in η or σ drops the coverage of the network. At $\sigma = 6$ dB the normalized distance of 0.1 can be reached with $\eta \approx 0.90$, however if σ is increased to 11 dB, then the same normalized distance can only be reached by $\eta \approx 0.45$ as shown in Fig. 5.3. This loss of QoS shows the effect of increasing the severity of shadowing on the network. Given a value of the SNR margin and the environments statistics in term of σ, an important question to be asked is, "what level of cooperation is optimal to have the maximum

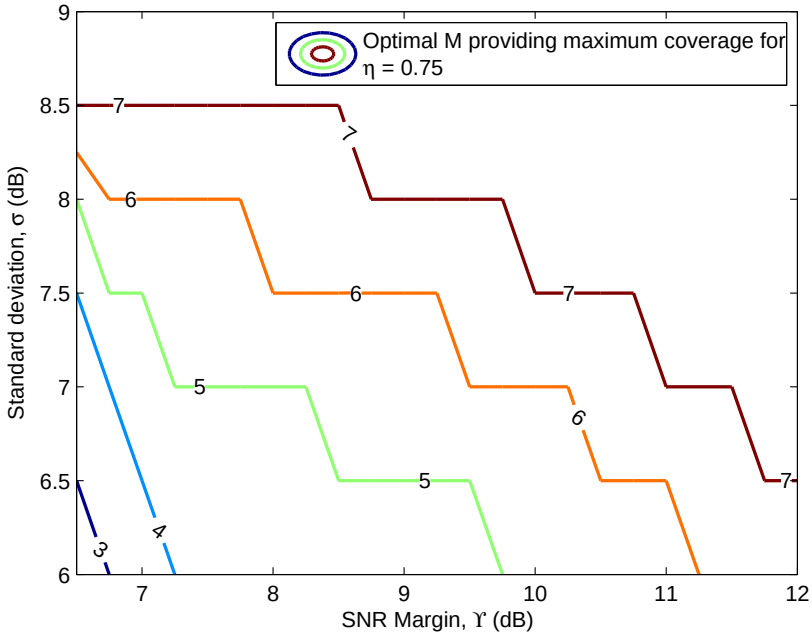

Figure 5.4: Optimal M for maximum coverage at $\eta = 0.75$.

coverage of the network and/or to have reliable hops?" In other words we are interested in finding the optimal value of M that yields maximum coverage for given channel conditions. Fig. 5.4. shows the contours of the optimal M, for $\eta = 0.75$, under various SNR margins and standard deviation of the shadowing. This result is obtained by first calculating the number of hops n_0 using (5.15) and then multiplying the number of hops n_0 by M to find the coverage. It can be noticed that when both σ and Υ are small, then a lower M will provide maximum coverage and vice versa. It can be seen that at $\sigma = 7$ dB and $\Upsilon = 8$ dB , the maximum coverage is obtained by selecting $M = 5$, however if σ is unchanged and the Υ is increased to 10 dB, then the maximum coverage is obtained by $M = 6$.

The results of Fig. 5.4. specifies the maximum coverage of the network,

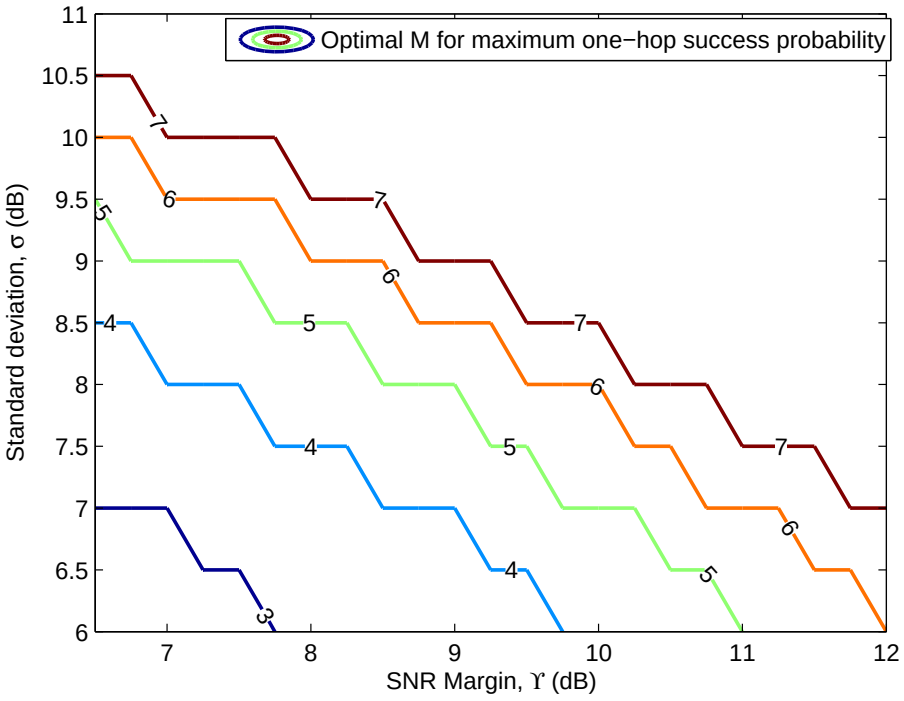

Figure 5.5: Optimal M for maximum probability of one-hop success ρ.

however, the individual hops may not be very reliable. For instance, η is just 75% for one-hop in Fig. 5.4. However, if reliable hops are required, then the level of cooperation may change for the same channel conditions. Fig. 5.5. shows the contours of the optimal M, which provide the maximum probability of one-hop success at different Υ and σ. It can be noticed from Fig. 5.5. that when $\Upsilon = 9$ dB and $\sigma = 7$ dB, then $M = 4$ give us the maximum $\rho = 0.9280$, however at the same parameters set, $M = 5$ provides the maximum coverage from Fig. 5.4. Similarly, for the same Υ, if σ is changed to 9 dB, then $M = 7$ will provide us the maximum probability of one-hop success, which is $\rho = 0.9722$. The results of Fig. 5.5. can be used in a broadcast scenario when more reliable hops are required at each broadcast phase, and it is required that each node must decode the message.

Fig. 5.6. shows the coverage of the network for three different channel models, i.e., fading, shadowing and composite shadowing-fading. The coverage is shown in terms of normalized distance at $M = 3$, $\Upsilon = 15$ dB, and $\eta = 0.90$. Three coverage behaviors are shown for shadowing and composite channel models at three different σ's. Since, fading is independent of σ, the result of fading channel is repeated with different results of shadowing and composite channel. The coverage of fading channel model has been obtained from [18]. It can be noticed that fading channel has the worst coverage when compared to shadowing and composite channels at $\sigma = 3$ dB. Shadow-only channel model provides the best coverage because of small $\sigma = 3$, introducing a macro-diversity effect. At $\sigma = 6$ dB, both the coverage of fading and shadowing are comparable while composite channel gives the worst performance. The coverage at $\sigma = 9$ dB is worst for composite shadowing-fading

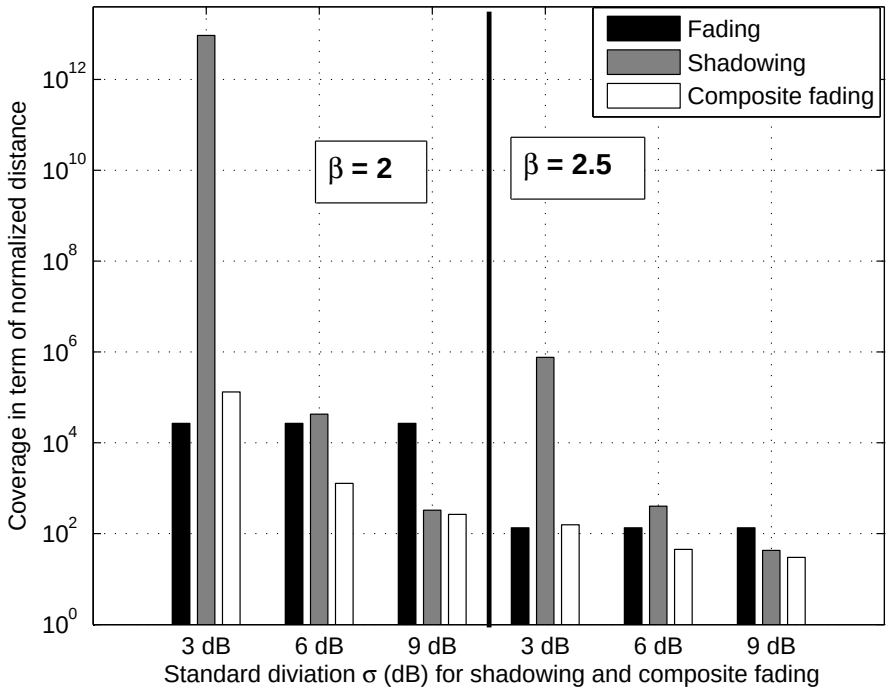

Figure 5.6: Coverage of the network under three different channel models.

while fading only channel provides the best performance. It can be seen that increasing the β from 2 to 2.5 does not change the trend of the coverage for the three channel models, however, the coverage of each channel model drops by increasing the path loss exponent. It can be inferred from the figure that within normal range of σ, i.e., 6-12 dB composite channel provides the lowest coverage as compared to fading and the shadowing channel model. Hence it is recommended to consider both the small-scale fading as well as shadowing while quantifying the performance of wireless networks.

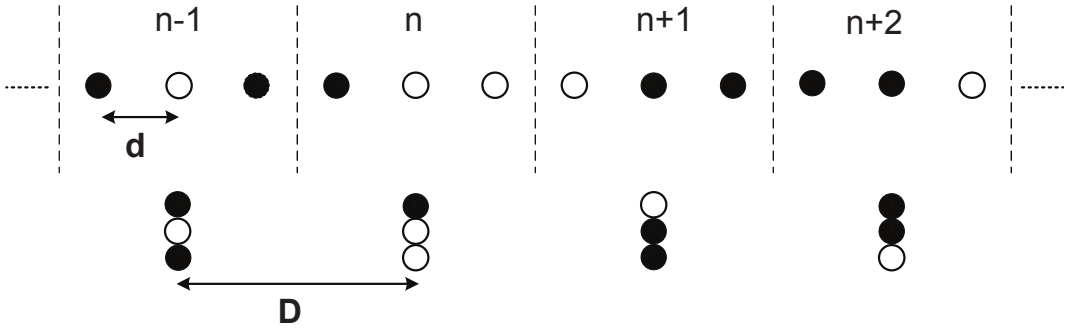

Figure 5.7: Co-lcated vs. equi-distant network topology.

5.3.1 Equi-Distant versus Co-located Network Topology

Fig. 5.7. shows the equi-distant and co-located network topologies for the line networks. In the co-located case, the nodes are placed close to each other [1] but the node density remains the same as that of the equi-distant topology. The hop distance of both the networks also remain equal.

Let ρ_D and ρ_d denote the probability of one-hop success for co-located and equi-distant network topologies, respectively. Fig. 5.8. shows the difference in the success probabilities of both the network topologies versus SNR margin at $\sigma = 6$ dB for various M. It can be noticed from the figure that at low Υ, the difference $(\rho_D - \rho_d)$ is negative, which shows that the equi-distant topology works better, and the difference become positive at the median range of Υ, which indicates that the co-located topology performs better in this region. At higher SNR margin, the performance of both the topologies become equal, which shows that a higher Υ has overcomed all the losses.

Fig. 5.9. shows the difference in the success probabilities of two topologies

[1] with at least half wavelength spacing for independent fading assumption to be valid

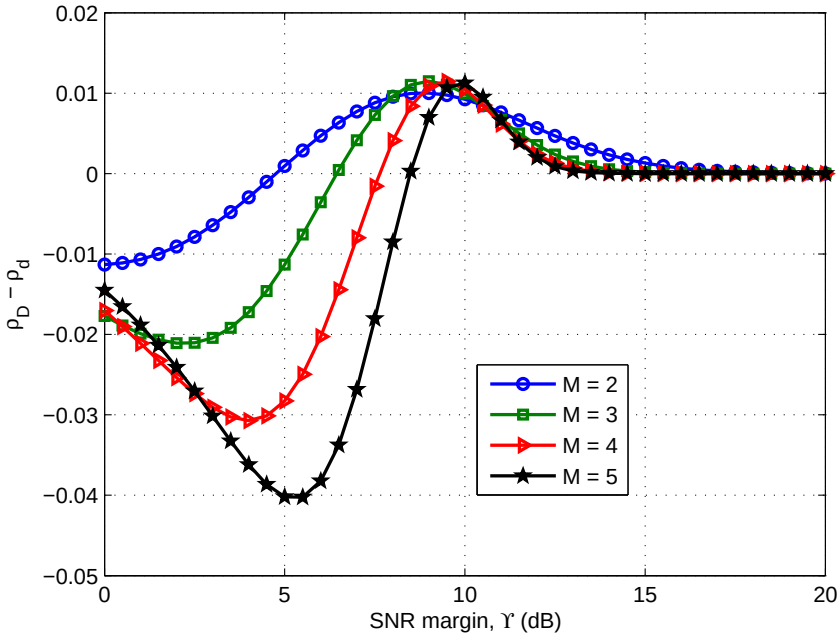

Figure 5.8: Difference in probability of one-hop success for two topologies; $\sigma = 6$ dB.

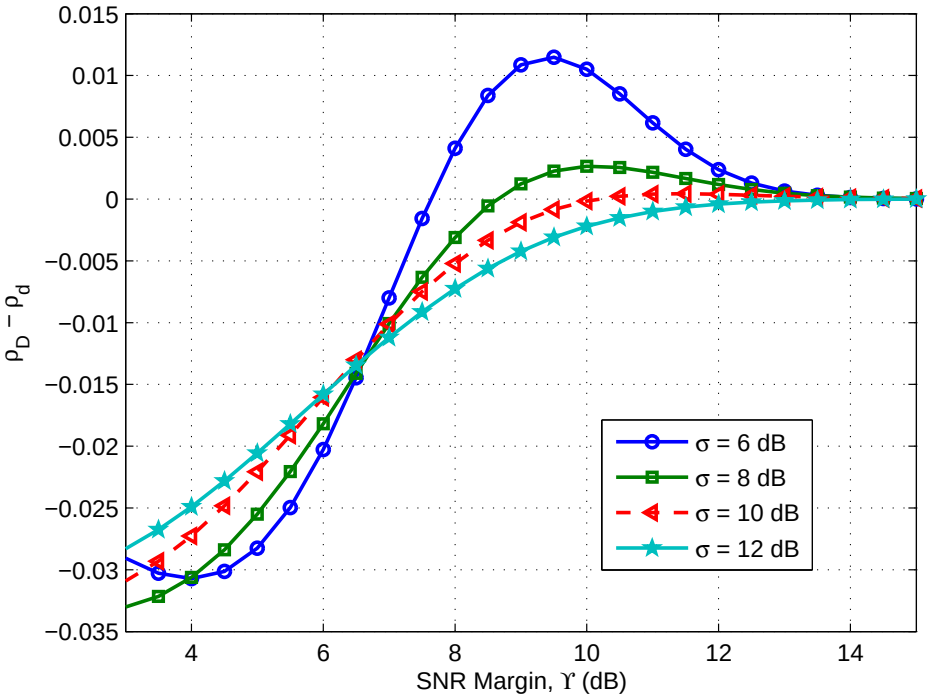

Figure 5.9: Effect of σ on the two network topologies; $M = 4$.

versus SNR margin at various values of σ while keeping $M = 4$ fixed. It can be seen that the equi-distant topology has better performance for almost the entire SNR range when the shadowing is severe. This result is contrary to [33], where it was shown that the co-located case always perform better if the channel exhibits small-scale fading only. As the σ is an environment dependent variable and Υ is a design parameter, a suggestion can be made to use a specific topology according to a specific channel model for better system performance.

Chapter 6

Conclusion and Future Work

6.1 Conclusion

A stochastic model for a cooperative multi-hop line network is presented. The transmission from one level to another is modeled as a quasi-stationary Markov process. The transition probability matrix of the Markov chain is derived by considering two different wireless channels, i.e., shadowing and composite shadowing-fading channel. Shadowing is modeled as a log-normal RV, while composite shadowing-fading is modeled as a Suzuki (Rayleigh-lognormal) RV. The sum distribution of the log-normal RVs is approximated by a single log-normal RV by using Fenton-Wilkinson's method. While sum of the multiple Suzuki RVs is approximated by an MGF-based technique, which uses the Gauss-Hermite integration to find the closed-form expression for the MGF of Suzuki and log-normal RVs. The coverage of the network for both channels is found by applying the Perron-Frobenius theory of non-negative matrices. The SNR margin required to achieve a certain quality of service under various system parameters has been quantified. The opti-

mal number of nodes in a level to give maximum coverage under composite shadowing-fading, for a given SNR margin and shadowing standard deviation has been quantified for a given QoS. The coverage of the same network for three different channels, i.e., fading, shadowing, composite shadowing-fading is compared for different system parameters. We found that composite channel severely limits the coverage of the networks. We recommend that in order to get the most practical results, one must consider both small-scale as well as large-scale fading. The choice of whether to use equi-distant or co-located topology under various system parameters has been presented for composite channel.

6.2 Future Directions

A possible future work is to incorporate multiple flows in the model and study the interference-limited performance of the network. The network model can be extended to a two-dimensional grid network. The non-overlapping assumption of our model can be relaxed and an overlapping level of nodes can be considered. A future work may be to study the random deployment of nodes. Synchronization among group of nodes is also an open area of research.

Bibliography

[1] G. J. Foschini and M. J. Gans, "On limits of wireless communications in a fading environment when using multiple antennas," *Wireless Pers. Commun.,* vol. 6, no. 3, Mar 1998, pp. 331-335

[2] J. N. Laneman, D. N. C. Tse, and G. W. Wornell, "Cooperative diversity in wireless networks: Efficient protocols and outage behavior," *IEEE Trans. Inf. Theory*, vol. 50, pp. 3062-3080, Dec. 2004.

[3] A. Sendonaris, E. Erlip. and B. Aazhang, "User cooperation diversity-part I: system description, *IEEE Trans. Commun.*, vol. 51, no. 11, pp. Nov. 2003.

[4] A. Sendonaris, E. Erlip. and B. Aazhang, "User cooperation diversity-part II: implementation aspects and performance analysis, *IEEE Trans. Commun.*, vol. 50, no. 11, pp. Nov. 2003.

[5] D. Wübben, "Cooperative communication in multihop networks," (Universitat Bremen), [online] 2012, http://www.ant.uni-bremen.de/en/projects/multihop/ (Accessed: 12 December, 2012)

[6] S. Ma, Y. Yang, and H. Sharif "Distributed MIMO technologies in cooperative wireless networks," *Advances in Cooperative Wireless Networking, IEEE Communication Magazine*, May 2011.

[7] A. Kailas and M. A. Ingram, "Alternating Opportunistic Large Arrays in Broadcasting for Network Lifetime Extension," *IEEE Trans. Wireless Commun.*, vol. 8, no. 6, pp. 2831-2835, June 2009.

[8] A. Scaglione and Y. W. Hong, "Opportunistic large arrays: Cooperative transmission in wireless multi-hop ad hoc networks to reach far distances," *IEEE Trans. Signal Process.*, vol. 51, no. 8, pp. 2082-92, Aug. 2003.

[9] A. Kailas and M. A. Ingram, "Alternating opportunistic large arrays in broadcasting for network lifetime extension," *IEEE Trans. Wireless Commun.*, vol. 8, no. 6, pp. 2831-2835, June 2009.

[10] S. A. Hassan and M.A. Ingram, "A quasi-stationary Markov Chain model of a cooperative multi-hop linear network, *IEEE Trans. Wireless Commun.*, vol. 10, no. 7, pp. 2306-2315, July 2011.

[11] S. A. Hassan and M.A. Ingram, "On the modeling of randomized distributed cooperation for linear multi-hop networks," in *IEEE Intl. Conf. Commun. (ICC)*, Ottawa, Canada, June 2012.

[12] S. A. Hassan and M. A. Ingram, "A stochastic approach in modeling cooperative line networks," in *IEEE Wireless Commun. Networking Conf. (WCNC),* Cancun, Mexico, March, 2011.

[13] S. A. Hassan, P. Wang, "Dual relay communication system: Channel capacity and power allocations, in *10th IEEE Intl. Wireless and Microwave Techn. Conf. (WAMICON)*, Clearwater, Fl., April 2009.

[14] S. A. Hassan, P. Wang, Y. G. Li, "Equalization for symmetrical cooperative relay scheme for wireless communications," in *11th IEEE Radio and Wireless Symposium (RWS)*, San Diego, CA, Jan. 2009.

[15] P. Wang, S. A. Hassan, Y. G. Li, "A symmetrical cooperative diversity approach for wireless communications," in *th IEEE Intl. Conf. on Circuits and Systems Commun. (ICCSC),* Beijing, China, May 2008.

[16] B. S. Mergen and A. Scaglione, "A continuum approach to dense wireless networks with cooperation," in *Proc. IEEE INFOCOM*, pp. 2755-2763, Mar. 2005.

[17] S. A. Hassan, "Range extension using optimal node deployment in linear multi-hop cooperative networks," in *IEEE Radio and Wireless Symposium (RWS)*, Austin, Texas, Jan. 2013.

[18] S. A. Hassan and M. A. Ingram, "Modeling of a cooperative one dimensional multi-hop network using quasi-stationary Markov chains," in *Proc. IEEE Global Commun. Conf. (Globecom)*, Miami, Fl., Dec. 2010.

[19] D. Kotz, C. Newport, R. S. Gray, J. Liu, Y. Yuan, and C. Elliott, "Experimental evaluation of wireless simulation assumptions," *Dartmouth Computer Science Technical Report*, TR2004-507, Jun. 2004.

[20] G. L. Stüber, *Principles of Mobile Communications*. 3rd Ed., Springer Publisher, 2011.

[21] T. S. Rappaport. *Wireless Communications: Principles and Practice.* 2nd ED., Pearson Education Publishers, 2009.

[22] Hirofumi Suzuki, "A statistical model for urban radio propagation," *IEEE Trans. Commun.*, vol. com-25, no. 7, July 1977.

[23] F. Graziosi and F. Santucci, " On SIR fade statistics in Rayleigh-lognormal channels," in *Proc. ICC*, pp. 1352-1357, 2002.

[24] L. F. Fenton, "The sum of lognormal probability distributions in scatter transmission systems," *IRE Trans. Commun. Syst.*, vol. CS-8, pp. 57-67, 1960.

[25] J. E. Tighe and T. T. Ha, "On the sum of multiplicative chi-square-lognormal random variables," in *Proc. Globecom*, pp. 3719-3722, 2001.

[26] N. B. Mehta, J. Wu, A. F. Molisch, and J. Zhang, "Approximating a sum of random variables with Lognormal," *IEEE Trans. Wireless Commun.*, vol. 6, no. 7, July 2007.

[27] C. Tellambura and A. Annamalai, "A unified numerical approach for computing the outage probability for mobile radio systems," *IEEE Commun. lett.*, vol. 3, pp. 97-99, 1999.

[28] M. Abramowitz and I. Stegun, *Handbook of Mathematical Functions with Formulas, Graphs, and Mathematical Tables.* Dover, 9 ed. 1972.

[29] A. A. Abu-Dayya and N. C. Beaulieu, "Outage probabilities in the presence of correlated lognormal interferers," *IEEE Trans. Veh. Technol.*, vol. 43, pp. 164-173, 1994.

[30] S. Schwartz and Y. Yeh, "On the distribution function and moments of power sums with lognormal components," *Bell Syst. Tech. J.*, vol. 61, pp. 1441-1462, 1982.

[31] C.D Meyer, *Matrix Analysis and Applied Linear Algebra,* SIAM publishers, 2001.

[32] E. A. van Doorn and P. K. Pollett, "Quasi-stationary distributions for reducible absorbing Markov chains in discrete time," *J. Markov Processes and Related Fields*, vol. 15, no. 2, pp. 191-204, 2009.

[33] S. A. Hassan and M. A. Ingram, "The benefit of co-locating groups of nodes in cooperative line networks," *IEEE Commun. Lett.*, vol. 16, no. 2, Feb. 2012.

[34] S. S. Szyszkowicz, H. Yanik. and J. S. Thompson, "On the feasibility of wireless shadowing correlation models," *IEEE Trans. Veh. Technol.*, vol. 59, no. 9, pp. 4222-4236 Nov. 2010.

[35] "Path loss and shadowing," best knowledge park, [online] 2013, http://bestknowledgepark.blogspot.com/2009/05/path-loss-and-shadowing.html (Accessed: 15 Feburary, 2013)

[36] T. Klingenbrunn and P. Mogensen, "Modeling cross-correlated shadowing in network simulations," in *Proc. IEEE VTC*, Sep.1999, vol. 3, pp. 1407-1411